Vol. 749: 109–125, 2024
https://doi.org/10.3354/meps14718

MARINE ECOLOGY PROGRESS SERIES
Mar Ecol Prog Ser

Published November 21

Quantifying the fates and retention of larval rockfish through Lagrangian analyses

Lucinda A. Quigley[1,*], Peter J. S. Franks[1], Andrew R. Thompson[2], John C. Field[3], Jarrod A. Santora[3,4]

[1]Scripps Institution of Oceanography, University of California San Diego, La Jolla, CA 92037, USA
[2]NOAA Fisheries Service, Southwest Fisheries Science Center, La Jolla, CA 92037, USA
[3]NOAA Fisheries Service, Southwest Fisheries Science Center, Fisheries Ecology Division, Santa Cruz, CA 95060, USA
[4]Department of Applied Math, University of California Santa Cruz, CA 95060, USA

ABSTRACT: Understanding larval transport pathways and retention is important for fisheries management and predicting recruitment variability. We investigated how mesoscale circulation patterns influence the retention and dispersal of larval rockfish *Sebastes* spp. within the California Current System off the western coast of the USA. Using a 25 yr record of satellite-derived geostrophic and Ekman velocity fields, Lagrangian particle tracking simulations were implemented to find pathways of passively drifting virtual particles representing rockfish larvae. Statistical fates of particles were averaged to reveal mean spatial and temporal patterns in retention and distance traveled. Yearly retention values were compared to observed pelagic juvenile rockfish abundance collected on annual surveys. Retention patterns varied spatially throughout the region, with the Southern California Bight emerging as a highly retentive region. Interannual variability in overall retention was positively related to the abundance of pelagic juvenile rockfish collected in the same year. Our analyses provide evidence supporting the successful implementation of the geographic placement of the Cowcod Conservation Areas, which were spatial closures implemented in the early 2000s to rebuild overfished rockfishes, and illustrate the utility of numerical simulations for understanding the retention and transport of pelagic larvae such as rockfish.

KEY WORDS: Marine protected area · Southern California · Recruitment · *Sebastes* spp.

1. INTRODUCTION

Understanding the suite of drivers that affect fish recruitment requires knowledge of the roles that physical mechanisms play in larval survival. Successful recruitment generally requires greater relative larval survival, as the larval stage of fishes is typically the life stage with the highest mortality rate (Hjort 1914, Houde 2008, Hare 2014). Due to the weak swimming abilities of the early life history stages of fishes, spatiotemporal variability of ocean currents can impact the distribution and survival of ichthyoplankton. Consequently, resolving larval transport is an important step toward understanding the influence of hydrodynamics on larval survival, in order to better predict fish distributions and recruitment.

Rockfish *Sebastes* spp. are ecologically and commercially important fishes found in the Northeast Pacific. There are more than 65 *Sebastes* species present along the western coast of the USA, with the greatest number of species found in the vicinity of the Southern California Bight (SCB; Love et al. 2002). Female rockfishes release internally hatched larvae (primitively viviparous). The majority of species (including the more abundant species) spawn during the winter, with larvae developing into pelagic juveniles after approx-

*Corresponding author: lquigley@ucsd.edu

Publisher: Inter-Research · www.int-res.com

imately 1–2 mo (Love et al. 2002). During their early larval period, rockfish exhibit weak swimming abilities and do not vertically migrate, essentially acting as passive particles drifting in the upper mixed layer, making their positioning highly susceptible to the influence of ocean currents (Moser & Boehlert 1991, Sakuma et al. 1999, Love et al. 2002, Stockhausen & Hermann 2007, Kashef et al. 2014). Following their larval stage, winter-spawning rockfish typically remain in the water column as pelagic juveniles for several months before settling out to either nearshore or shelf habitats, at which point they are typically referred to as settled juveniles. Depending on the species, this juvenile stage will typically last for several to many years, with adult life spans ranging from approximately a decade to up to a century or more for some species (Love et al. 2002).

During the late 1990s and early 2000s, 7 rockfish species were declared to be overfished, with expected recovery times ranging several decades due to the species' slow growth, late maturity, high longevity, and generally low productivity (Berkeley et al. 2004). This led to management responses to reduce fishing mortality, including spatial habitat closures. Marine protected areas called Cowcod Conservation Areas (CCAs) were established in the SCB with the intent of protecting habitat for the cowcod *Sebastes levis*. The CCAs comprised 2 separate regions encompassing a total surface area of approximately 11 138 km^2. While the CCAs were implemented primarily to help rebuild cowcod, other rockfish species benefited from the reserves (Hitchman et al. 2012, Thompson et al. 2016, 2017, Fennie et al. 2023). These conservation areas were established based on historical catch records of cowcod and prohibited bottom contact fishing at depths greater than 20–40 fathoms (~36–73 m; depth closure regulations were modified slightly over time) to minimize cowcod fishing mortality (Butler et al. 2003, Dick & He 2019). These closures, coupled with a broad suite of additional management measures implemented to rebuild depleted populations, were highly successful, as the cowcod stock was declared as rebuilt in 2019, following earlier rebuilding success of 5 of the initial 7 rockfish species declared to be overfished. Consequently, most regulations that implemented spatial closures to protect overfished rockfishes were removed in 2023, including most protections within the CCAs. As of January 2024, commercial trawling is prohibited within the CCAs, while fixed gear and recreational fisheries are allowed.

While the CCAs were recognized as critically important for the recovery of the cowcod population, it is important to recognize that high adult catch records alone do not necessarily coincide with locations or habitats conducive for larval survival (Shen et al. 2017) and, subsequently, recruitment, which is needed to maintain population growth. Marine protected areas that are located in regions where larvae are produced but are then advected to unfavorable habitats may be less effective than if the protected areas were located in zones where locally produced larvae are transported to ecologically favorable areas (White et al. 2014). Marine reserves should also supply larvae to zones accessible to fishing (Pelc et al. 2010, Hitchman et al. 2012). Thus, determining the placement of marine reserves benefits from the identification of transport pathways of larvae and retention hotspots (Stockhausen & Hermann 2007, Petersen et al. 2010, Hitchman et al. 2012, Andrews et al. 2021).

Larval transport models are useful tools for fisheries management and marine reserve planning (Lett et al. 2006, Stockhausen & Hermann 2007, Petersen et al. 2010, Andrews et al. 2021, Mori et al. 2022). Petersen et al. (2010) used numerical simulations of particle transport to investigate larval rockfish transport patterns in a narrow coastal region in central California. Their work illustrated the utility of simple numerical simulations in understanding the transport pathways of rockfish in the California Current System (CCS). More recently, Morales (2023) used particle tracking to show that ocean current patterns can facilitate the recruitment of shortbelly rockfish *S. jordani* in central California.

The CCS is an eastern boundary upwelling system, characterized by high biological production and dynamic oceanographic conditions (Checkley & Barth 2009, Bograd et al. 2019). The California Current brings cool, low-salinity, high-oxygen, and high-nutrient water from the north toward the equator. Warmer, higher-salinity water forms the California Undercurrent, which flows northward near shore and is centered at a depth of ~100 m, although its depth can range from 500 m to the surface (Zaba et al. 2021). Coastal wind-driven upwelling brings deep, cold, saline, low-oxygen, and nutrient-rich waters to the surface at the coast, enhancing primary production along the coast. Surface Ekman transport is directed offshore, driving coastally upwelled waters into waters that are more oligotrophic and associated with lower production. In the CCS, the physical environment varies with both seasonal wind-driven upwelling and interannual climate variations such as the El Niño–Southern Oscillation and the Pacific Decadal Oscillation (Checkley & Barth 2009).

Ichthyoplankton distributions are impacted by temporal variability in upwelling and ocean circulation, coupled with the timing of fish spawning. Spawning

in the winter, when wind-driven offshore Ekman transport is weakest, is one strategy to minimize advection offshore (Parrish et al. 1981, Giddings et al. 2022). Cross-shore transport of larvae to offshore oligotrophic regions may have negative consequences for fish survival and recruitment (Nieto et al. 2014, Morales 2023). Nearshore retention of rockfish larvae may facilitate survival through increased prey availability and delivery of larvae to viable adult habitats, including marine protected areas (Caselle et al. 2010, Petersen et al. 2010).

Our objective was to quantify the fates of rockfish larvae released in central and southern California—the epicenter of rockfish diversity (Love et al. 2002). Lagrangian particle tracking simulations, forced by a 25 yr record of remotely sensed geostrophic and Ekman velocity fields, were used to track passively drifting virtual particles representing rockfish larvae. Spatial and temporal patterns of larval rockfish transport were quantified by metrics including the fraction of larvae retained inshore of the 2000 m isobath, net distance traveled, gross distance traveled, and the net-to-gross displacement ratio. We also examined particle advection into and away from the CCAs in the SCB and investigated connectivity of the CCAs. Finally, we examined the relationship between simulated interannual larval retention and observed annual pelagic juvenile abundance patterns derived from a fisheries-independent ecosystem assessment survey. Our analyses provide novel insights into rockfish larval transport and retention, with important implications for the ongoing management of these commercially and ecologically important species.

2. MATERIALS AND METHODS

2.1. Study location

Virtual particles representing rockfish larvae were randomly seeded throughout the study domain, and placements on land were avoided. The domain was defined by the coastline and the 2000 m isobath and spanned from the SCB (~30.5° N) in the south to Monterey Bay (~37° N) in the north, with the northern and southern boundaries of the domain constructed approximately perpendicular to the coastline (Fig. 1). Although the highest densities of most winter-spawning rockfishes are in benthic habitats between approximately 100 and 500 m depth, the offshore extent of the domain was chosen based on observations of high abundances of rockfish larvae out to the 2000 m isobath (Moser & Boehlert 1991, Thompson et al. 2016). Bathymetry data was obtained from the ETOPO Global Relief Model (NOAA National Centers for Environmental Information 2022).

2.2. Particle tracking

On each day from 1–31 January, 1000 virtual particles were seeded at random locations within the defined domain (Fig. 1). Particles were tracked forward in time for 30 d using a time step of 1 d. The simulations were performed every year for 25 yr (1998–2022), resulting in a total of 775 000 particle trajectories. Although most rockfish have a spawning season that may span several months during late fall, winter, and sometimes early spring, January typically represents the month of greatest larval release for most species (Moser & Boehlert 1991).

We chose a simulation duration of 30 d based on rockfish larval stage duration. Larval and pelagic

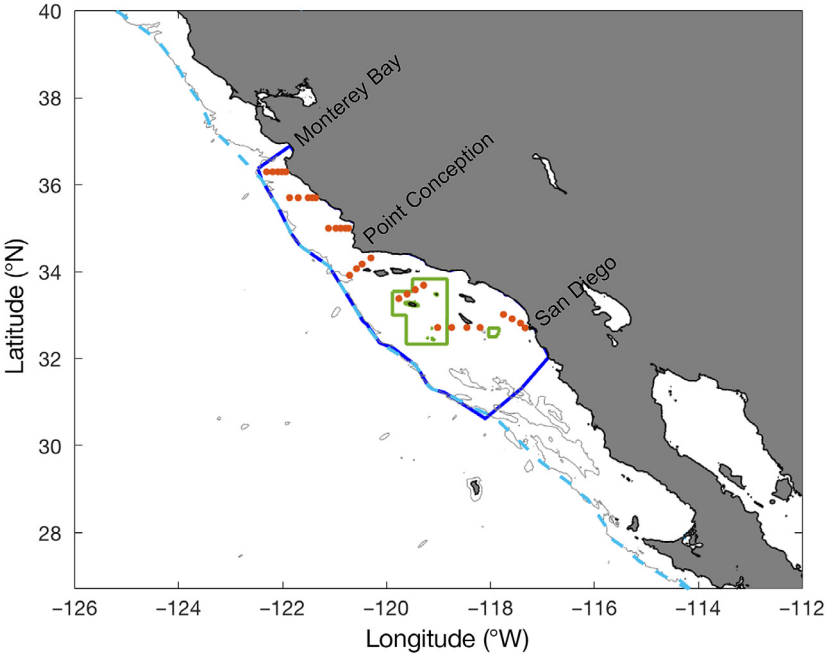

Fig. 1. Study region in California. Dark blue line: domain where rockfish larval particles were seeded; light blue dashed line: offshore boundary that defines retention for the final locations; light gray lines: 2000 m isobath; green boxed outlines: Cowcod Conservation Areas; orange markers: Rockfish Recruitment and Ecosystem Assessment Survey sampling locations used in this study. The high-resolution coastline in all figures is for visualization purposes only

juvenile stage duration varies among rockfish species, but for winter-spawning species, the larval stage typically lasts 1–2 mo, with the pelagic juvenile stage lasting another 3–4 mo, after larvae have undergone flexion and adopted meristic counts associated with adult stages (Love et al. 2002, Ralston et al. 2013, Kashef et al. 2014). Pre-flexion rockfish larvae are characterized by poor swimming ability (0.5–1.8 cm s^{-1}); however, swimming ability increases rapidly with body size, with pelagic juveniles capable of swimming 8.6–53.5 cm s^{-1} (Kashef et al. 2014). Pelagic juveniles are thus capable of outswimming some horizontal surface currents, suggesting that implementing forward-in-time particle tracking on rockfish older than 30 d may not be suitable. We conservatively defined a larval period of 30 d and assumed that rockfish within 30 d of parturition act as passively drifting particles, as other works have done (Petersen et al. 2010, Nishimoto et al. 2019).

Eulerian velocity fields at a given location were linearly interpolated from 0.25° gridded velocity data to estimate the particle's velocity at any arbitrary location. Given initial locations (x,y) at time (t), new particle locations (forward in time) can be found by the first-order Euler scheme. A random walk term representing horizontal diffusivity was added (Batchelder 2006), so the equation for forward-in-time particle tracking with spatially constant diffusivity was:

$$\begin{aligned} x(t+\Delta t) &= x(t) + u(x,y,t)\times\Delta t + \sqrt{2K_{\mathrm{H}}\Delta t}\times Q \\ y(t+\Delta t) &= y(t) + v(x,y,t)\times\Delta t + \sqrt{2K_{\mathrm{H}}\Delta t}\times Q \end{aligned} \quad (1)$$

where u and v are horizontal and vertical velocities, Q is a Gaussian random variable with a zero mean and unit variance, and K_{H} is the horizontal diffusivity. A value of 26 m^2 s^{-1} was selected for K_{H}, where $K_{\mathrm{H}} = (2.06 \times 10^{-4}) \times L^{1.15}$, with L referring to the length scale of diffusion; in our case, the ~28 km resolution of the velocity data used (Okubo 1970, Matsuzaki & Fujita 2017).

The velocity fields used to force the simulations do not resolve coastal flows well, so we assume that particles that were advected close to shore would become controlled predominantly by finer-scale coastal dynamics that are outside the scope of this work. We implemented a boundary at the coastline where velocities become 0 m s^{-1} and used a re-drifting operation as defined by Kataoka et al. (2013). If a particle ended up on land during the simulation, the particle was returned to its location from the previous time step, and this operation was repeatedly performed in each time step (Kataoka et al. 2013). As a sensitivity analysis, we also conducted simulations using a time step of 1 h; however, we found no significant difference in particle advection, so we opted to use daily time steps for computational efficiency. Furthermore, we compared simulations releasing 1000 and 10 000 particles per day and found no significant differences between yearly mean retention or spatial distribution of final particles, so we chose 1000 particles. Figs. S1 & S2 illustrate the results of the sensitivity analyses and can be found in the Supplement at www.int-res.com/articles/suppl/m749p109_supp.pdf.

2.3. Satellite-derived velocity fields

Geostrophic velocity fields used to generate larval trajectories were derived from satellite-estimated sea-surface height (SSH) anomalies through the Copernicus Marine Environment Monitoring Service[1]. We used daily geostrophic velocities with a wind-driven Ekman component at 15 m, available at a 0.25° (~28 km) resolution. Ekman currents were modeled using European Centre for Medium-Range Weather Forecasts ERA5 wind stress (Rio et al. 2014). We also performed simulations using only geostrophic velocity fields to assess the role of Ekman currents in our particle trajectories. Although the 2-dimensional geostrophic and Ekman currents do not completely resolve the fine-scale complexity of currents, geostrophic and Ekman flows are the dominant components at the larger spatial and temporal scales we investigated (Parrish et al. 1981, Dong et al. 2021). We did not investigate vertical motions in our analyses. Rockfish larvae are found in the upper 80 m of the water column and show no evidence of vertical migration, making them well suited for simulations that are forced by horizontal geostrophic and Ekman velocity fields (Moser & Boehlert 1991, Sakuma et al. 1999, Love et al. 2002).

The satellite-derived velocities are based on measurements of SSH anomalies. SSH anomalies are a result of the vertical distribution of density throughout the water column below. The SSH anomalies are used to generate horizontal geostrophic surface currents from the horizontal pressure gradients and Coriolis. Using the satellite-derived geostrophic and 15 m Ekman velocities gives velocity fields representative of the upper ~100 m of the water column, with

[1]Global total (COPERNICUS-GLOBCURRENT), Ekman and geostrophic currents at the surface and 15 m. E.U. Copernicus Marine Service Information (CMEMS). Marine Data Store (MDS). https://doi.org/10.48670/mds-00327 (accessed 16 August 2023)

a weak contribution from the wind. We opted to use satellite-derived velocities instead of a hydrodynamic model. Models can accurately reproduce average ocean properties such as eddy kinetic energy. However, in comparisons of regional ocean models and satellite data, we found that the models we investigated did not accurately reproduce the locations and intensities of individual mesoscale features — and it is those features that are central to our investigations of larval transport. For the focus of this paper, which is recreating specific dispersal pathways of larvae, we determined that satellite-derived velocities were the best tool for exploring the influences of horizontal advection of rockfish larvae in mesoscale circulations in the SCB.

2.4. Rockfish fates

We classified each particle as 'retained' based on whether its final location was inshore of the 2000 m isobath (Fig. 1). Habitats shallower than 2000 m bottom depth are likely to be within swimming distance of habitat suitable for the settlement of pelagic juveniles, while habitats deeper than 2000 m bottom depth represent distant offshore areas from which pelagic juveniles would be unlikely to reach their adult habitat closer to shore. Particles that traveled north or south out of the seeding domain but remained inshore of the 2000 m isobath were thus included in the retained category.

For each particle, we computed the gross distance traveled (distance calculated over every daily time step and summed) and net distance traveled (distance calculated from seeding to final location). The net-to-gross displacement ratio, calculated as net distance divided by gross distance, was used to understand the degree of linearity of the particle trajectories. High net-to-gross displacement ratios indicate linear paths, while low net-to-gross displacement ratios indicate more meandering trajectories, potentially indicative of eddies.

We calculated time-averaged geostrophic and geostrophic + Ekman 15 m velocities by computing the mean velocity magnitude and direction for each 0.25° × 0.25° grid cell throughout the months of January and February across all 25 yr to assess mean flow and differences between the 2 velocity products. We also calculated the average wind speed at 1000 hPa during January and February across all 25 yr to illustrate the role of the wind-driven Ekman velocity component. Wind data were obtained from ECMWF Reanalysis v5 (ERA5) monthly averaged data (Hersbach et al. 2023).

To assess temporal variability in retention, we calculated the fraction of particles that remained inshore of the 2000 m isobath after 30 d for each year and across all years combined. As a model evaluation exercise, we compared predicted yearly retention to observed pelagic juvenile rockfish abundance to assess the relationship between retention and survival to the pelagic young-of-the-year (YOY) stage. We used YOY rockfish abundance indices derived from the Rockfish Recruitment and Ecosystem Assessment Survey (RREAS; Fig. 1). This fixed-station survey collects 3–4 mo old pelagic YOY rockfish off California using a midwater trawl (target depth: 30–40 m) and has been conducted in the late spring each year since 1983 (Ralston et al. 2013). Importantly, this is the time frame when larvae spawned in the winter would become pelagic juveniles. Since 2004, the survey effort has expanded to include the entire US West Coast, including the SCB (Field et al. 2021). We used RREAS data from 2004–2022 and analyzed pelagic YOY rockfish abundances from stations between 36.3° and 32.7° N, the region encompassing the south-central and southern regions of the survey (Fig. 1). For each year, we calculated the arithmetic mean YOY rockfish abundance among all stations. We then performed *Z*-score normalization to standardize abundances to a mean zero and unit standard deviation. We compared rockfish yearly retention with abundance for 2004–2022, excluding 2011 and 2020 due to reduced RREAS sampling in those years (Santora et al. 2021).

To investigate spatial variability in retention, we calculated the number of particles seeded within each 0.25° × 0.25° grid cell that were subsequently retained inshore of the 2000 m isobath, divided by the total number of particles seeded within that grid cell. To visualize the results, we mapped rockfish particle distributions. To account for varying shelf width throughout the study region, we computed the least-cost distance to shore for each grid cell (shortest distance from each grid cell to the nearest coastline grid cell). If distance to the coast explained the spatial patterns of retention, then we would expect that particles seeded farther from shore would be less likely to end up retained inshore of the 2000 m isobath, and particles seeded close to shore would be more likely to be retained. We multiplied the fraction of particles retained by the least-cost distance to shore for each grid cell to determine whether proximity to the coast could explain the spatial variability in the fraction retained. If the retention fraction was inversely related to the distance to the coast, then we would expect to see a relatively homogeneous distribution of the multiplication product, as small retention fractions

would be multiplied by large distances, and large retention fractions would be multiplied by small distances. Similarly, we performed the same analysis using distance to the 2000 m isobath instead of distance to the coast. For this case, we divided retention by distance to the 2000 m isobath, as locations close to the boundary would likely have low retention, and locations far from the boundary would have high retention.

We also explored the transport pathways of particles that were seeded specifically within the CCAs. We examined both the final distributions of particles seeded in the CCAs as well as the seeding locations of particles that ended up in the CCAs. The fraction of particles retained was calculated as the number of particles that were seeded within the CCAs that remained inshore of the 2000 m isobath, divided by the total number of particles that were seeded within the CCAs.

3. RESULTS

3.1. Velocity product evaluation

Temporally averaged geostrophic and geostrophic + Ekman 15 m velocities over 25 yr (1998–2022) were similar (Fig. 2a,b). While the Ekman component was minimal in winter in the CCS due to weak winds, it added a weak southwest flow component to the geostrophic velocities (Fig. 2c). At equilibrium, surface Ekman currents are directed 45° to the right of the wind vector in the Northern Hemisphere, and total Ekman transport is directed 90° to the right of the wind vector. Ekman currents at 15 m were directed between 45° and 90° to the right of the wind vector. The southwestern flow attributed to the Ekman 15 m velocity component aligned with expectations, given the mean wind vectors which were strongly directed to the southeast (Fig. 2d).

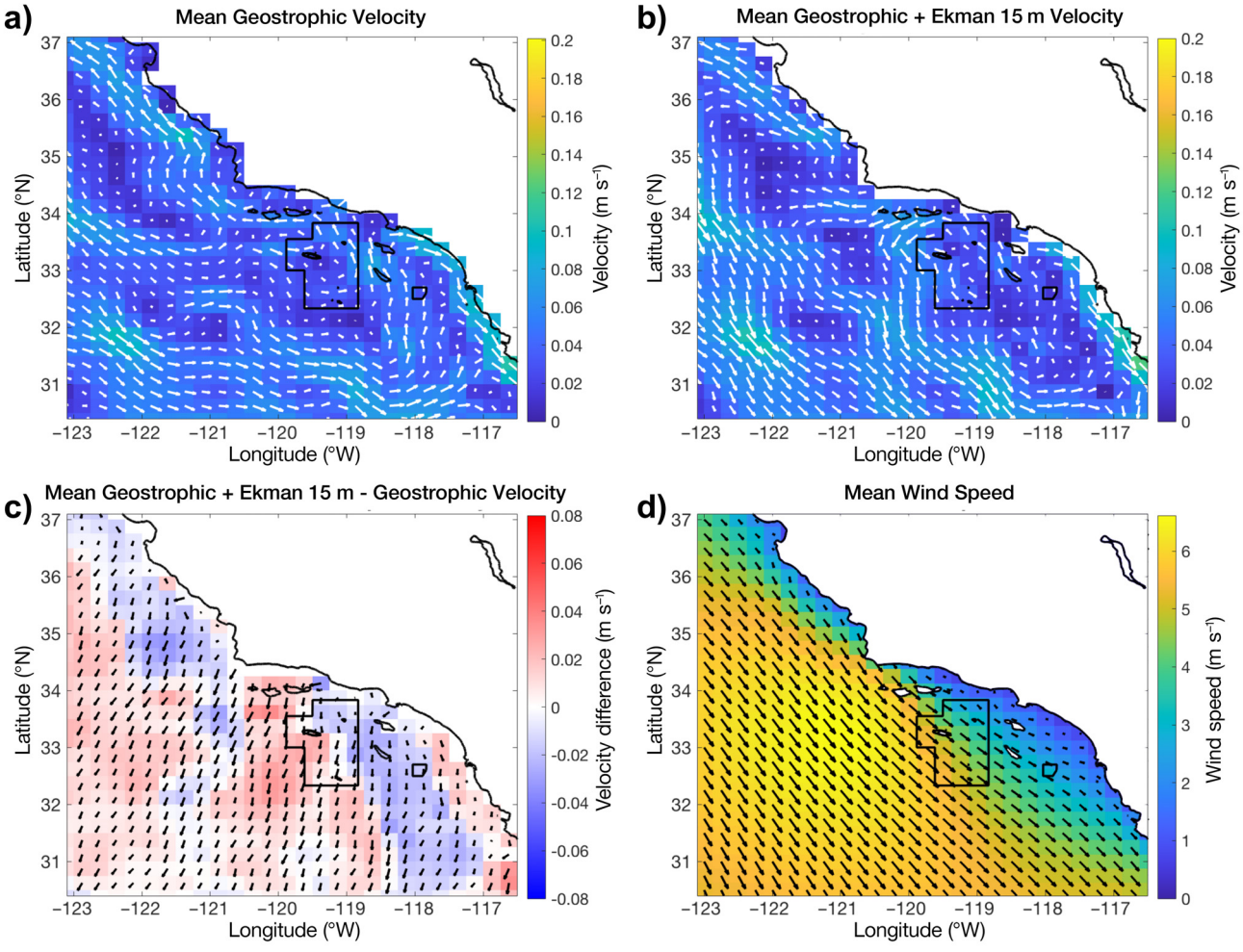

Fig. 2. Average velocities over 25 yr during January and February for (a) geostrophic velocities; (b) geostrophic + Ekman 15 m velocities; (c) average geostrophic + Ekman 15 m velocities minus average geostrophic velocities (b − a); and (d) 25 yr average wind speed during January and February at 1000 hPa. Black boxed outlines: Cowcod Conservation Areas. Arrows are scaled according to the magnitude represented in the colors

North of Point Conception (~34° N), there was strong northward flow along the coast that was part of a cyclonic circulation pattern. South of Point Conception, in the center of the SCB, flows appeared more chaotic and weaker in and around the Channel Islands. Off San Diego (32.5° N, 117° W), the temporally averaged velocities appeared strong and directed southward.

We opted to analyze the particle tracking simulations forced by geostrophic + Ekman 15 m velocities: the focus of our work is to determine offshore transport, and the Ekman currents can play a large role in advecting particles offshore. The particle distributions were similar between both velocity products, with the simulations using geostrophic + Ekman 15 m velocities resulting in particle distributions shifted southeast compared to the simulations forced by geostrophic velocities (Fig. S3). We include the results of the particle tracking simulations using geostrophic currents in Figs. S4–S6 & Table S1 the Supplement.

3.2. Particle tracking and rockfish fates

The final locations of particles after 30 d spanned from 27° –40° N, and from the coast to well offshore of the 2000 m isobath, up to 570 km from the coast. Particles spread relatively evenly northward and southward, with the farthest particle extending beyond the seeding domain 385 km north and 398 km south. Maps of the final locations reveal greater concentrations of particle final locations within the seeding region and enhanced concentrations in the SCB (Fig. 3).

Spatial patterns of mean net and gross distance traveled by particles were similar. Particles seeded near the 2000 m isobath were advected farther in terms of both net and gross distance traveled. Minimum distances traveled were found near the coast and within the SCB (Fig. 4a,b). The mean net-to-gross displacement ratio was highest in the SCB, along the coast near San Diego (Fig. 4c). This high net-to-gross displacement is consistent with particles seeded in this region traveling relatively linearly. In contrast, other regions in the interior of the SCB showed lower net-to-gross displacement ratios, consistent with more tortuous trajectories.

The fraction of larvae retained was highest in the SCB, close to the coast (Fig. 5). The spatial patterns of the fraction retained were not perfectly inversely related to the distance to the coast or to the 2000 m isobath (Fig. 5). In general, retention was highest close to the coast and far from the 2000 m isobath (Fig. 6). For a given distance both to the coast and to the 2000 m isobath, there was a range of retention values associated with that distance (Fig. 6). Distance to the 2000 m isobath explained more of the variability in retention than distance to coast, with a trend of increasing retention with increasing distance to the 2000 m isobath. The R^2 values of a cubic polynomial fit to retention and distance to shelf, and retention and distance to coast were 0.84 and 0.22, respectively. However, right at the boundary of the 2000 m isobath

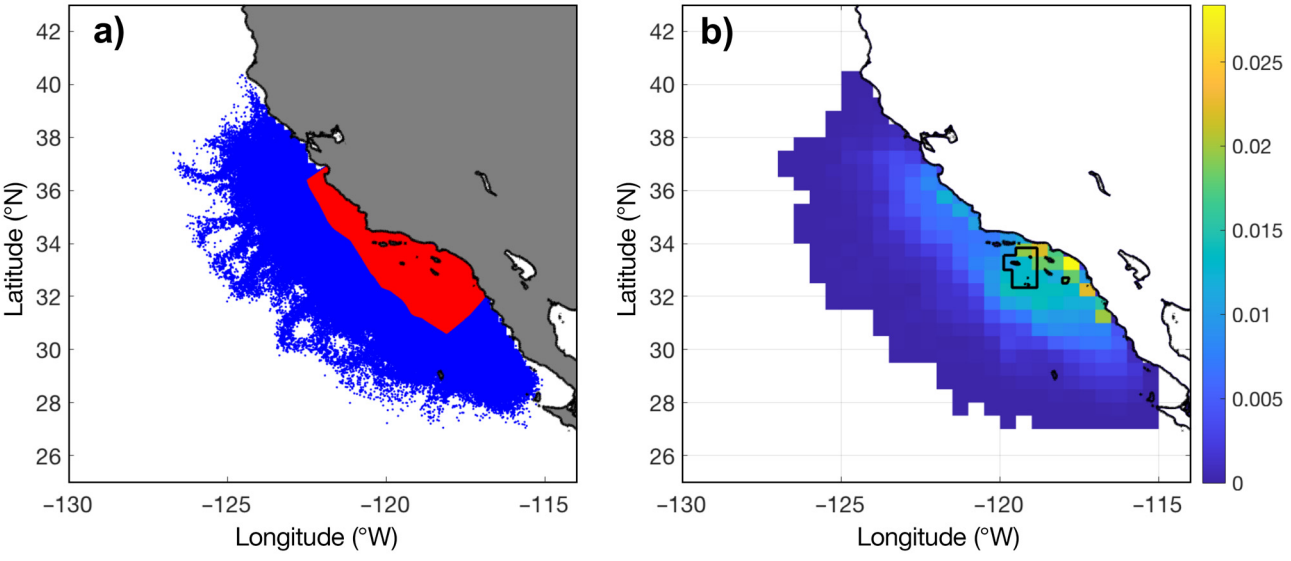

Fig. 3. (a) Seed locations of all rockfish larval particles (red) and final locations of all particles after 30 d advection (blue); (b) distributions of final locations of all particles; color corresponds to the percentage of total particles found in that grid cell

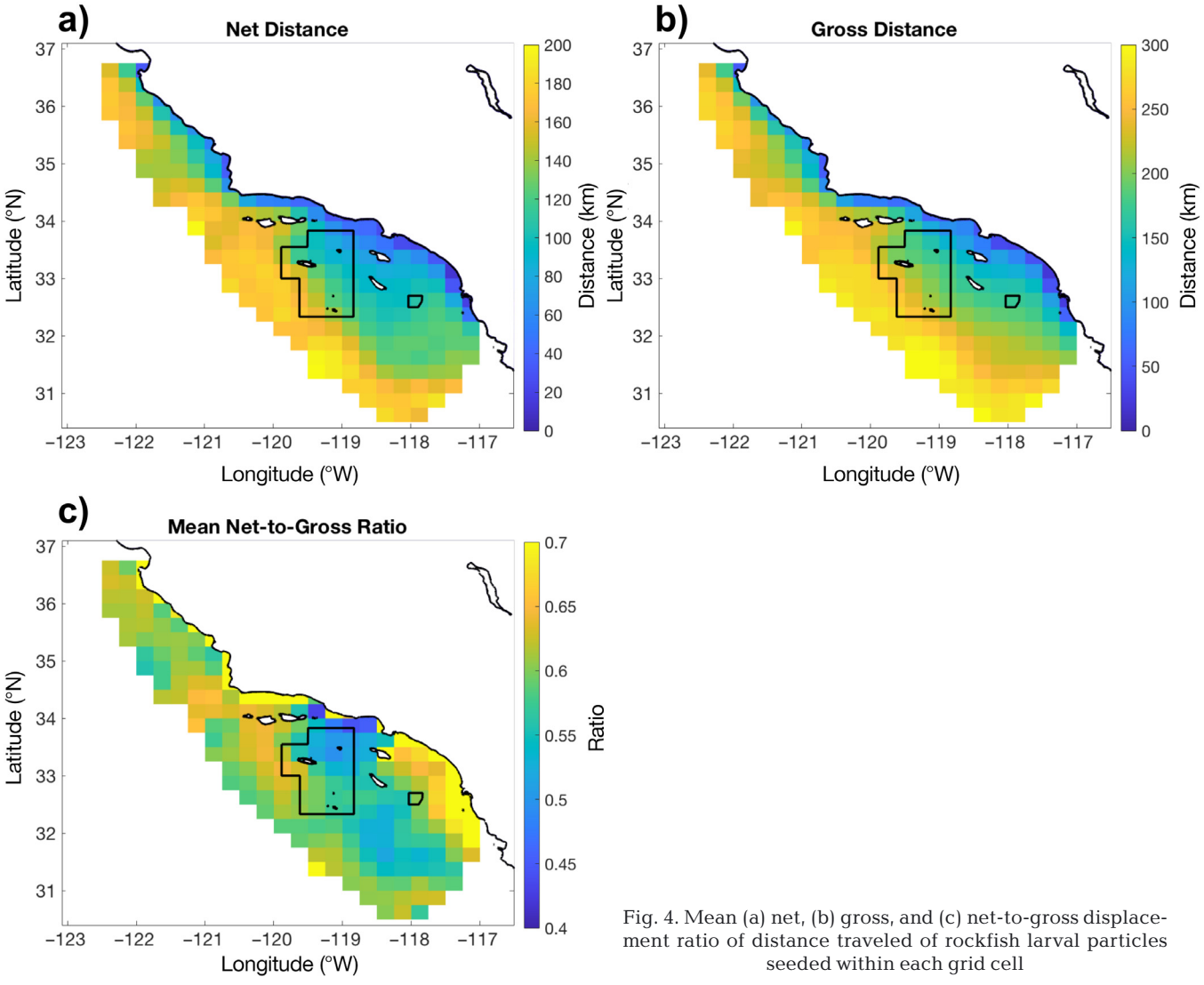

Fig. 4. Mean (a) net, (b) gross, and (c) net-to-gross displacement ratio of distance traveled of rockfish larval particles seeded within each grid cell

(0 km away), there was still a range of 0.39 in retention values, indicating that proximity to geographic boundaries does not explain all of the variability in retention.

The fraction of particles retained across all years was 0.71 (Table 1). Interannual variability in retention ranged from 0.51 to 0.86. Distributions of particles that started or ended in the CCAs revealed specific patterns of transport associated with these regions. Particles seeded in the CCAs were primarily transported southeast (Fig. 7a), although there was also a relatively high fraction of particles that were transported north and northeast to coastal habitats. Across all years combined, 19% of particles seeded in the CCAs ended up in the CCAs after 30 d. Of particles seeded outside of the CCAs, 5% of them were advected into the CCAs. Particles that ended in the CCAs after 30 d originated most frequently within the CCA and SCB (Fig. 7b). Regions south of the CCAs sourced particles to the CCAs more than regions north of the CCAs, with minimal contributions (0.1% of the particles that ended up within the CCAs) originating from north of Point Conception (Fig. 7b). These observations align with the patterns of mean flow; Point Conception delineates a boundary in flow, with particles that originated north of this topographic feature likely to be advected north or west but not south (Fig. 2).

Yearly larval retention values were higher during observed high YOY abundance years (mean standardized abundances greater than 0) than during low YOY years (mean standardized abundances less than 0; Fig. 8). High YOY abundance years occurred

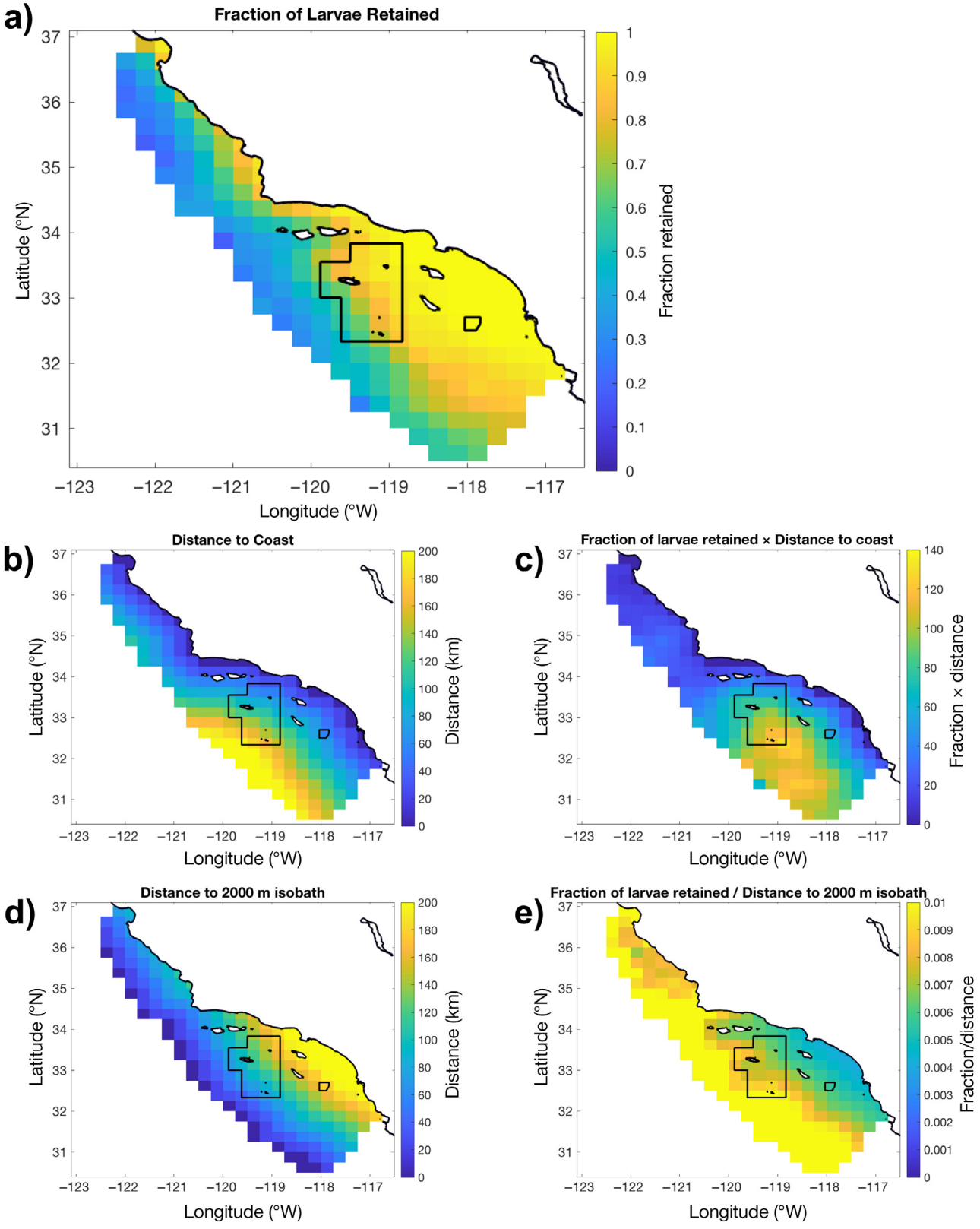

Fig. 5. (a) Fraction of rockfish larvae seeded within each 0.25° × 0.25° grid cell that were retained inshore of the 2000 m isobath; (b) distance to coast for each 0.25° × 0.25° grid cell; (c) fraction of larvae retained multiplied by distance to coast; (d) distance to 2000 m isobath for each 0.25° × 0.25° grid cell; and (e) fraction of larvae retained divided by distance to 2000 m isobath

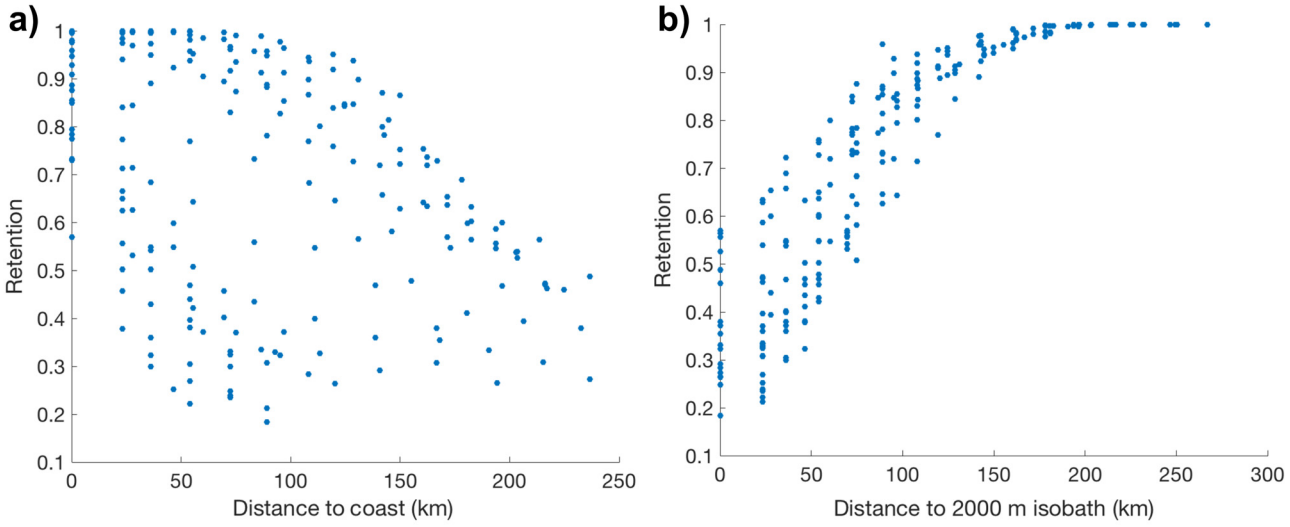

Fig. 6. Retention of rockfish larval particles vs. (a) distance to the coast and (b) distance to the 2000 m isobath

Table 1. Fraction of rockfish larvae retained inshore of the 2000 m isobath for each year and all years combined. Geostrophic + Ekman 15 m velocity fields were used to force the simulations

Year	Fraction retained	Year	Fraction retained
1998	0.82	2011	0.74
1999	0.71	2012	0.64
2000	0.86	2013	0.71
2001	0.77	2014	0.71
2002	0.67	2015	0.74
2003	0.68	2016	0.73
2004	0.69	2017	0.8
2005	0.75	2018	0.65
2006	0.65	2019	0.79
2007	0.71	2020	0.58
2008	0.76	2021	0.62
2009	0.76	2022	0.51
2010	0.75	All years	0.71

during 2005, 2010, and 2013–2017 (Fig. 8a). Years of high YOY abundances were only associated with high retention values, while years of low YOY abundances corresponded to a wider range of retention values, including lower values. High YOY abundance years had retention fractions ranging from 0.71 to 0.80, while low juvenile abundance years corresponded to retention values ranging from 0.51 to 0.79 (Fig. 8b). Retention values were significantly different between years of high and low juvenile abundance (*t*-test, $t = -2.213$, $p = 0.047$).

4. DISCUSSION

We investigated the spatial and temporal variability of larval rockfish transport and retention using a Lagrangian particle tracking model to assess scales of variability over 25 yr. We evaluated our model with fishery-independent observations of juvenile rockfish abundance and found that higher recruitment coincides with higher retention rates. The numerical simulations and summary statistics illustrate the potential dynamics of rockfish larval transport during winter, revealing differences across biogeographic provinces that are separated by a coastal promontory and highlighting the importance and success of previous conservation and fishery management areas. Our simulations and analyses serve as relatively simple tools to increase our understanding of the role of mesoscale ocean circulation and retention patterns on larval success and, ultimately, recruitment.

4.1. Temporal patterns of transport

Larval survival and recruitment are functions of hydrodynamic and biological factors across many temporal and spatial scales (Houde 1987, 2008, Hare 2014). The dominant components of flow relevant to our study of month-long passive advection of larvae were geostrophic and Ekman velocities (Parrish et al. 1981). Although wind-driven upwelling and Ekman transport are minimal in the winter in the CCS (Chelton et al. 2007), Ekman velocities still contribute a flow component directed to the southwest

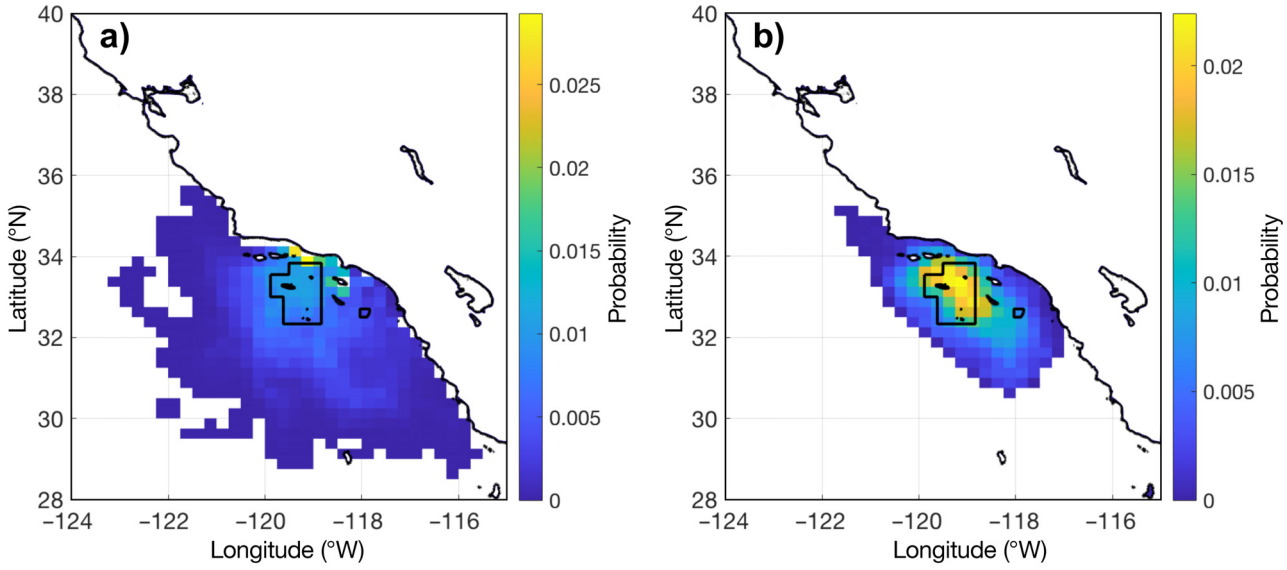

Fig. 7. Distributions of (a) final locations of rockfish larval particles that started in the Cowcod Conservation Areas and (b) seed locations of particles that ended in the Cowcod Conservation Areas

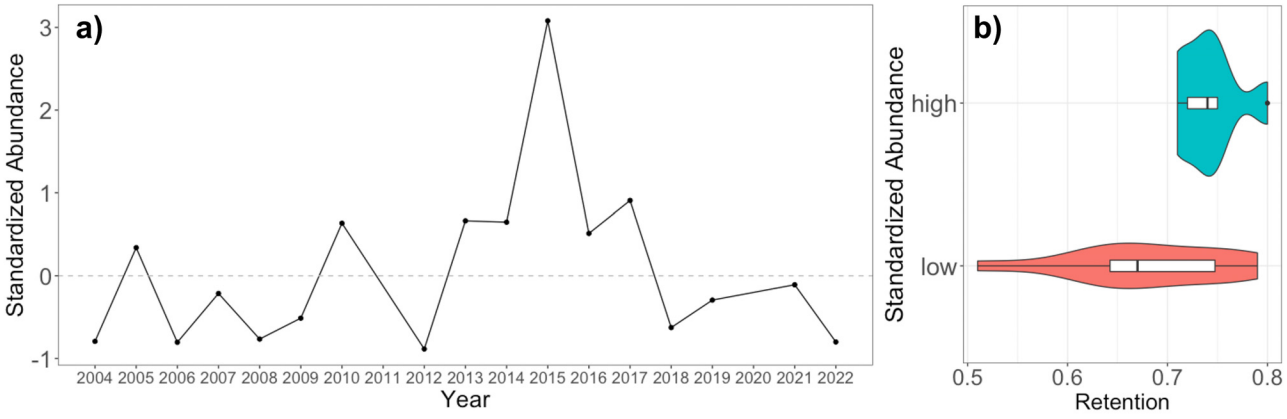

Fig. 8. (a) Rockfish pelagic young-of-the-year standardized abundance over 2004–2022; (b) violin plots with inset boxplots illustrating retention values for high versus low abundance years. Boxplots display the 25th, median, and 75th percentiles. High and low abundances are defined by mean standardized abundances greater than 0 and less than 0, respectively

(Fig. 2). One life history strategy to minimize advection offshore is spawning during the winter, when upwelling and offshore transport is weak (Parrish et al. 1981, Taylor et al. 2004, Giddings et al. 2022). Even with the inclusion of Ekman velocities, our simulations suggest a high degree of overall retention of larvae in the winter; this suggests that the effect of Ekman flow is not strong enough during January and February to counteract the geostrophic currents. Retention varied interannually, and in all years, a majority of larvae released were retained inshore of the 2000 m isobath after 30 d. The years with the lowest retention (2020 and 2022) had mean velocities within the study region with a significant westward component: northwest and southwest, respectively (294°, 0.025 m s^{-1} and 241°, 0.024 m s^{-1}; Fig. 9). The highest retention years (1998 and 2000) had weak mean velocities or eastward components: southeast and south (142°, 0.030 m s^{-1} and 180°, 0.00064 m s^{-1}; Fig. 9). A strong offshore component leads to less retention due to the offshore transport of larvae.

4.2. Spatial patterns of transport

Our analyses support the idea that the SCB is a highly retentive region within central and southern California waters (Taylor et al. 2004). The retention and transport of larvae depended on the location of

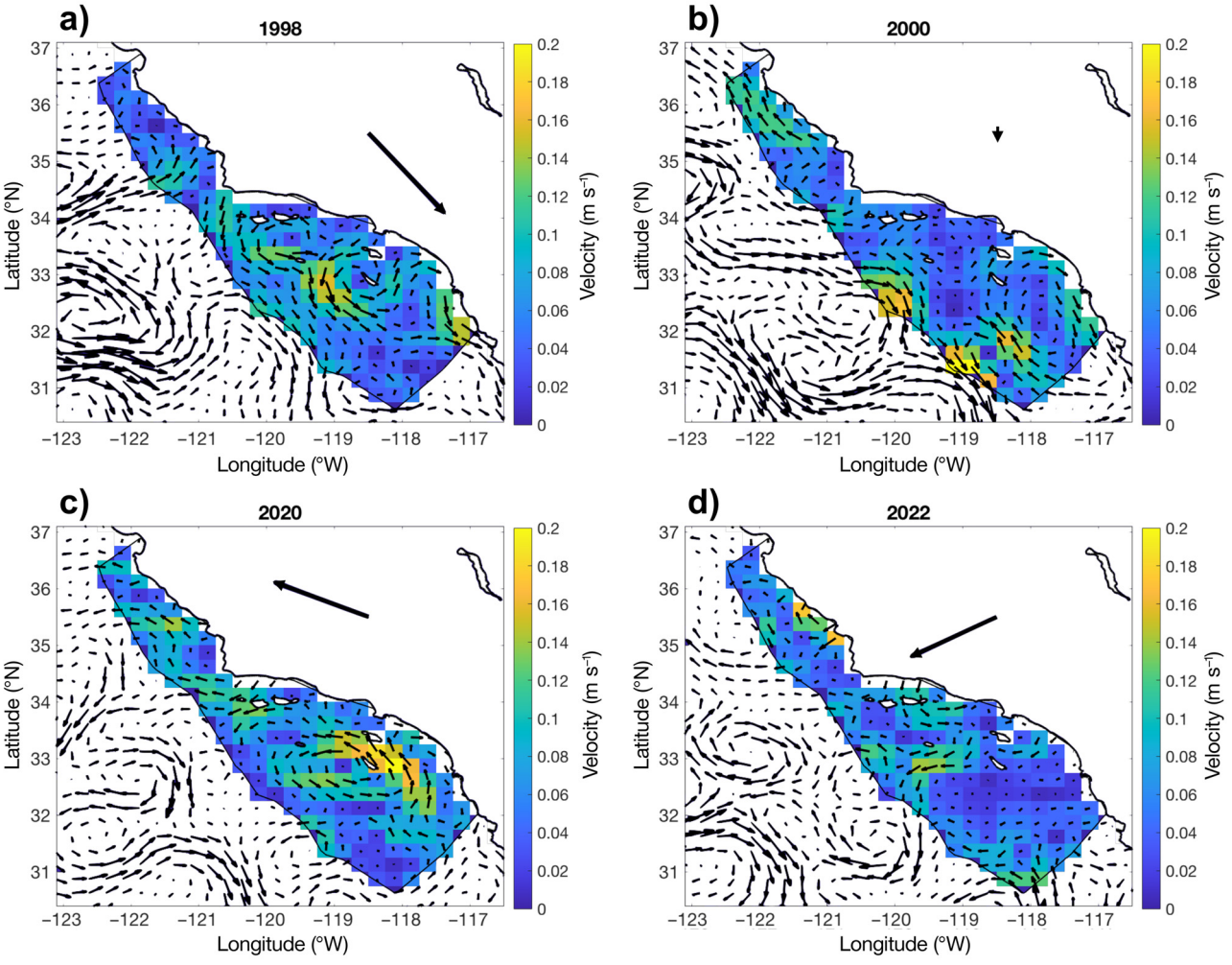

Fig. 9. Mean geostrophic + Ekman 15 m currents from the first 61 d of each year, (corresponding with the days used in the rockfish larval particle tracking simulations) for (a,b) the 2 years with the highest retention, and (c,d) the 2 years with the lowest retention. Black arrows: direction of the mean velocity in the study region, scaled by magnitude

the initial release site. The spatial patterns of the net-to-gross displacement ratio reflect patterns observed in the time-averaged current velocities. The region with the highest mean net-to-gross displacement ratio was found along the coast of San Diego (between 31° to 33° N and 118° to 119° W), where strong mean flows were directed persistently to the south. High net-to-gross displacement ratios were also observed southeast of Point Conception (~34° N), where strong westward flows dominated the mean velocity field, as well as along the coast north of Point Conception where northward velocities were strong and relatively free of eddies and meanders. In the interior of the SCB, the low net-to-gross displacement ratios corresponded to the weak and chaotic flow patterns characteristic of the interior of the Southern California Eddy. The Southern California Eddy is a semi-persistent feature in the SCB. It is present from July through January and is less prominent from February through May, with periodic dissolution of the eddy most frequently occurring in April (Owen 1980, Lynn & Simpson 1987). Eddies can retain larvae (Owen 1980, Fiedler 1986, Nishimoto & Washburn 2002, Bakun 2006, Nishimoto et al. 2019). Thus, the Southern California Eddy may facilitate larval retention (Taylor et al. 2004), as evidenced by the low net-to-gross displacement ratios and high retention of particles seeded in the interior of the SCB. Conversely, the high net-to-gross displacement ratios off San Diego may be attributed to its mean southward transport and being located outside of the Southern California Eddy (Mitarai et al. 2009). In addition to Ekman transport being weakest in the winter, our analyses suggest that the stability of the Southern California

Eddy in the winter is another characteristic of the hydrodynamic field that makes spawning in the winter advantageous.

The variability in the fraction of particles retained was not explained solely by the distance to the coast or distance to the 2000 m isobath, suggesting that interannual spatial variability in ocean circulation patterns influenced the resulting retention patterns. Fennie et al. (2023) found that rockfish larvae that were collected farther from fishing ports and in years when mothers were exposed to Pacific Subarctic (California Current) water were born larger—an indicator of larval condition. Larvae that are born farther from fishing ports, such as those in the CCAs, may be in better condition due to a greater relative abundance of larger, older spawning females (due to less fishing pressure) and may benefit from habitat conditions including the colder, low-salinity characteristics of Pacific Subarctic Upper Water (Miller et al. 2014, Schroeder et al. 2019, Fennie et al. 2023). Our analyses identified where larvae were both more likely to be born in good condition (farther from shore) and more likely to be retained (higher retention). The intersection of locations that are both far from the coast and have high retention suggest a mesoscale hotspot location within the SCB (high values in Fig. 5c), where larvae are likely to be in better condition and also remain inshore of the 2000 m isobath (Fennie et al. 2023). This hotspot slightly overlaps with the CCAs, although the core of the hotspot is south of the designated protected areas (Fig. 5c). Our analyses also revealed the larger CCA as a high retention area, given its proximity to both the coast and the 2000 m isobath (Fig. 5c,e). These findings have important management implications, as conserving quality habitat relies on understanding the location and size of optimal areas from a number of different perspectives, including but not limited to retention and quality of larvae (Caselle et al. 2003, White et al. 2014).

Our analyses underscore Point Conception as a topographic feature that defines a significant transition in the flow and the resulting larval transport. Point Conception has been recognized as a major biogeographic boundary that separates the region into distinct circulation patterns (Gaylord & Gaines 2000, Checkley & Barth 2009, Gottscho 2016). Dispersal, growth, and connectivity of many planktonic organisms are affected by this oceanographic feature (Gaylord & Gaines 2000, Blanchette et al. 2007). The southward-flowing California Current separates from the coastline as it passes Point Conception (Hickey 1979). This divergence of flow forms the semi-persistent cyclonic Southern California Eddy (Owen 1980). We found that larvae originating north of Point Conception were unlikely to be transported into the CCAs within the SCB (Fig. 7b). Similarly, Field et al. (2021) found that pelagic YOY rockfish abundance in the SCB varied out of phase from abundance trends between Point Conception and Cape Mendocino to the north. Moreover, Nishimoto et al. (2019) conducted particle-tracking simulations of larvae released from oil platform sites in the SCB and found that the potential for larvae to travel from southern locations to northern locations was greater than the potential for larvae to move from north to south. The CCAs, therefore, are sources of larvae that likely remain primarily within the SCB. Ideally, marine reserves should be strategically placed in locations where larvae are produced and dispersed to other nearby regions, while also reseeding the reserves with new adults (Pelc et al. 2010, Hitchman et al. 2012, Andrews et al. 2021). While our analyses cannot reveal where more mobile pelagic YOY rockfish will settle, the transport patterns show that larvae seeded in the CCAs are primarily retained inshore of the 2000 m isobath and transported to regions adjacent to the CCAs (Fig. 7a). These findings suggest that the placement of the CCAs was favorable from a spatial management perspective, as larvae born in the CCAs would seed surrounding regions, including coastal areas more accessible to fishing. Previous work has illustrated the effectiveness of the CCAs by showing that these marine protected areas are associated with higher abundances, species richness, and enhanced diversity of rockfish species (Hitchman et al. 2012, Thompson et al. 2016, Freeman et al. 2022). The effectiveness of the CCAs is likely a function of both habitat and circulation as well as reduced fishery removals due to their distance from port (Miller et al. 2014). Lagrangian particle-tracking simulations provide a new source of evidence supporting the placement of these spatial management areas, adding context to their success in both maintaining and rebuilding rockfish populations in this region by virtue of their role in reseeding both the CCAs as well as adjacent areas that remained open to fishing during the period of rockfish rebuilding.

4.3. Relationship between retention and recruitment

Density-independent environmental processes drive most of the variability in year-class strength of marine fishes, including rockfish, during the first 30 d of their life (Johnson 2006, Houde 2008, Field et al. 2010, Ral-

ston et al. 2013), and these processes likely include ocean circulation patterns (Hjort 1926). Pelagic YOY abundances in central and southern California increased beginning in 2013 and remained high throug hout the marine heatwave of 2014–2016 (Wells et al. 2017, Schroeder et al. 2019, Field et al. 2021). We hypothesized that retention of larvae, driven by ocean circulation, would be positively correlated with recruitment to the pelagic juvenile stage. If more larvae were retained, the abundance of larvae surviving to the juvenile stage would likely be higher. We tested this hypothesis by comparing interannual retention probabilities to abundances of YOY rockfish collected on the continental shelf 3–4 mo after being born. In our study, there was not a single high-abundance year during years of low retention. Low abundances that occurred during years of high retention were very likely due to other factors, such as greater starvation or predation mortality, poor temperature regimes, or factors related to food availability (Houde 2008, Hare 2014, Morales 2023, Swalethorp et al. 2023). In other words, retention appears to be an important factor in determining the potential for high juvenile abundances several months later. While other works have illustrated the importance of the environment and physical flow to rockfish juvenile abundances (e.g. Ralston et al. 2013, Schroeder et al. 2019), our simulations of larval transport directly link larval retention and juvenile abundances by identifying the mechanism responsible.

Recruitment is a complex function of hydrodynamic and trophodynamic factors that operate at various spatial and temporal scales (Houde 2008, Caselle et al. 2010). Even if rockfish larvae are advected offshore, pelagic juveniles are competent swimmers and may be capable of returning shoreward by moving deeper in the water column where flow is directed onshore (Lenarz et al. 1991). Indeed, this likely occurred in 1999 when pelagic YOY abundance in central California was low but very large year classes were observed in the fisheries for nearly all rockfish species a few years later (Field et al. 2010, Ralston et al. 2013, Stachura et al. 2014). Therefore, while it is unlikely that juvenile abundance is solely a function of larval retention, our results suggest that retention is often a critical prerequisite to successful recruitment.

4.4. Limitations

Our analyses provide insight into larval transport and retention, with larvae randomly seeded throughout the entire study region to investigate potential transport. However, to comprehensively understand transport, we require a finer-scale understanding of the spatial distributions and variability of larval rockfish spawning areas. If locations that we identified as having large fractions of larvae retained do not have a high number of larvae being produced there, these locations will not necessarily be important hotspots of retention or recruitment. Future work should take into account spatial variations in larval production to gain a better understanding of hotspots for production and associated retention (Taylor et al. 2004).

Future work would also benefit from a greater exploration of how larval transport and retention vary seasonally. Although the winter months are the peak of spawning activity for most winter-spawning rockfish, spawning can take place from mid-fall through the spring for most species, with many of the winter-spawning rockfish in this region spawning multiple times during favorable environmental conditions (Lefebvre et al. 2018, Holder & Field 2019, Beyer et al. 2021). Other work has shown that particle-dispersal patterns show strong seasonality in the SCB, and releases of particles just weeks apart can lead to different trajectories (Mitarai et al. 2009). A greater understanding of the extent to which the advection and retention patterns observed in the SCB represent the entire spawning season would be beneficial in developing quantitative metrics to inform future recruitment studies; however, this was beyond the scope of this research effort.

We used satellite-derived velocity products to force our particle-tracking simulations. For the mesoscale motions that we are interested in, satellite-derived velocities enable a synoptic understanding of the mesoscale patterns of flow (Parrish et al. 1981). Additionally, because rockfish larvae tend to be found in the upper layer of the ocean and, importantly, show no evidence of vertical migration (Sakuma et al. 1999), they are well suited for simulations that use satellite-derived geostrophic and Ekman velocities, which resolve the upper water column. Petersen et al. (2010) conducted numerical simulations to investigate rockfish transport along the central California coast. They used the Regional Ocean Modeling System and tracked particles along 5 different isobaths, from 1–70 m. The particles tracked in the winter showed coherent patterns of transport at all depths and aligned with our observations of northward particle transport of particles released in central California (Petersen et al. 2010).

A limitation of satellite-derived current velocities is that they do not accurately reproduce near-coastal dynamics. Smaller-scale components of flow that likely affect larval transport, such as nearshore and

tidal processes (Pineda 1991), are not examined here. Nearshore flows are more complex than the open-ocean currents that we use here and are influenced by a number of different processes such as buoyancy-driven flows, boundary-layer effects, bathymetry, and surface gravity waves (Pineda et al. 2007). We focused our analyses on large spatial scales spanning southern and central California and from the coast to the 2000 m isobath. Thus, our analyses are applicable for understanding broad trends and patterns in retention and transport, but we caution against interpreting our results on a finer scale. Moreover, coarse velocity field resolutions, such as the resolution used here, have been shown to result in higher retention of particles nearshore (Dauhajre et al. 2019). Away from the coast, satellite-derived velocities may overestimate eddies and underestimate particle dispersal driven by submesoscale flows (Sinha et al. 2019). Additional work using higher-resolution velocity fields (e.g. SWOT; Morrow et al. 2019) should focus on disentangling the finer-scale dynamics of rockfish larval transport in specific regions, although even with higher-resolution velocity fields, retention may still be overestimated (Sinha et al. 2019). Regions of interest to focus future studies on are the nearshore coastal region, the CCAs, and the recently created Groundfish Exclusion Areas (8 areas south of Point Conception implemented to protect sensitive habitats; PFMC 2023).

4.5. Conclusions

Disentangling the relationships between larval survival, hydrodynamic factors, and biological factors remains a primary challenge in fisheries oceanography (Hare 2014). The relative importance of physical and biological influences on larval survival has been a topic of debate for over a century, and the answers continue to be elusive (Hjort 1914, Houde 1987, 2008, Cury & Roy 1989). Here, we provide novel insights into rockfish larval transport. Our simple Lagrangian simulations showed that larval retention varies spatially and temporally, driven by differing physical conditions. We found that the SCB is a highly retentive region, owing to its mesoscale circulation patterns and the presence of the Southern California Eddy. Our methods can be applied to species other than rockfishes that have similar passive pelagic larval stages to understand larval retention and dispersal. Larval retention is a driving factor in setting recruitment strength, with higher retention acting as a prerequisite to high pelagic YOY abundance and ultimate year-class strength within adult populations. Moreover, our analyses highlight the efficacy of the design of the CCAs, providing new supporting evidence that their geographic placement was effective for the broad dispersal of successful recruits. While a wide array of additional biological and physical forcings play complex roles with respect to survival and dispersal of the early life stages of fishes, our work resolving transport pathways greatly enhances our understanding of the role of hydrodynamics on larval success and recruitment.

Acknowledgements. We thank the captains, officers, and crew of the NOAA ships and chartered survey vessels that made the pelagic juvenile rockfish data collections possible, as well as the many scientists and volunteers who participated and otherwise supported these surveys. We also thank 3 anonymous reviewers for their insightful comments that improved the manuscript.

LITERATURE CITED

Andrews K, Bartos B, Harvey CJ, Tonnes D, Bhuthimethee M, MacCready P (2021) Testing the potential for larval dispersal to explain connectivity and population structure of threatened rockfish species in Puget Sound. Mar Ecol Prog Ser 677:95–113

Bakun A (2006) Fronts and eddies as key structures in the habitat of marine fish larvae: opportunity, adaptive response and competitive advantage. Sci Mar 70(Suppl 2): 105–122

Batchelder HP (2006) Forward-in-time-/backward-in-time-trajectory (FITT/BITT) modeling of particles and organisms in the coastal ocean. J Atmos Ocean Technol 23: 727–741

Berkeley SA, Hixon MA, Larson RJ, Love MS (2004) Fisheries sustainability via protection of age structure and spatial distribution of fish populations. Fisheries 29: 23–32

Beyer SG, Alonzo SH, Sogard SM (2021) Zero, one or more broods: reproductive plasticity in response to temperature, food, and body size in the live-bearing rosy rockfish *Sebastes rosaceus*. Mar Ecol Prog Ser 669:151–173

Blanchette CA, Helmuth B, Gaines SD (2007) Spatial patterns of growth in the mussel, *Mytilus californianus*, across a major oceanographic and biogeographic boundary at Point Conception, California, USA. J Exp Mar Biol Ecol 340:126–148

Bograd SJ, Schroeder ID, Jacox MG (2019) A water mass history of the Southern California current system. Geophys Res Lett 46:6690–6698

Butler JL, Jacobson LD, Barnes JT, Moser HG (2003) Biology and population dynamics of cowcod (*Sebastes levis*) in the southern California Bight. Fish Bull 101:260–280

Caselle JE, Hamilton SL, Warner RR (2003) The interaction of retention, recruitment, and density-dependent mortality in the spatial placement of marine reserves. Gulf Caribb Res 14:107–117

Caselle JE, Kinlan BP, Warner RR (2010) Temporal and spatial scales of influence on nearshore fish settlement in the Southern California Bight. Bull Mar Sci 86:355–385

Checkley DM, Barth JA (2009) Patterns and processes in the California Current System. Prog Oceanogr 83:49–64

Chelton DB, Schlax MG, Samelson RM (2007) Summertime coupling between sea surface temperature and wind stress in the California Current System. J Phys Oceanogr 37:495–517

Cury P, Roy C (1989) Optimal environmental window and pelagic fish recruitment success in upwelling areas. Can J Fish Aquat Sci 46:670–680

Dauhajre DP, McWilliams JC, Renault L (2019) Nearshore Lagrangian connectivity: submesoscale influence and resolution sensitivity. J Geophys Res Oceans 124:5180–5204

Dick EJ, He X (2019) Status of cowcod (*Sebastes levis*). Pacific Fishery Management Council, Portland, OR

Dong H, Zhou M, Hu Z, Zhang Z, Zhong Y, Basedow SL, Smith WO Jr (2021) Transport barriers and the retention of *Calanus finmarchicus* on the Lofoten Shelf in early spring. J Geophys Res Oceans 126:e2021JC017408

Fennie HW, Ben-Aderet N, Bograd SJ, Kwan GT, Santora JA, Schroeder ID, Thompson AR (2023) Momma's larvae: maternal oceanographic experience and larval size influence early survival of rockfishes. Fish Oceanogr 33: e12658

Fiedler PC (1986) Offshore entrainment of anchovy spawning habitat, eggs, and larvae by a displaced eddy in 1985. CCOFI Rep 27:144–152

Field JC, MacCall AD, Ralston S, Love MS, Miller EF (2010) Bocaccionomics: the effectiveness of pre-recruit indices for assessment and management of bocaccio. CCOFI Rep 51:77–90

Field JC, Miller RR, Santora JA, Tolimieri N and others (2021) Spatiotemporal patterns of variability in the abundance and distribution of winter-spawned pelagic juvenile rockfish in the California Current. PLOS ONE 16: e0251638

Freeman JB, Semmens BX, Thompson AR (2022) Impacts of marine protected areas and the environment on larval rockfish species richness and assemblage structure in the Southern California Bight. Mar Ecol Prog Ser 698:125–137

Gaylord B, Gaines SD (2000) Temperature or transport? Range limits in marine species mediated solely by flow. Am Nat 155:769–789

Giddings A, Franks PJS, Baumann-Pickering S (2022) Monthly to decadal variability of mesoscale stirring in the California Current System: links to upwelling, climate forcing, and chlorophyll transport. J Geophys Res Oceans 127:e2021JC18180

Gottscho AD (2016) Zoogeography of the San Andreas Fault system: Great Pacific Fracture Zones correspond with spatially concordant phylogeographic boundaries in western North America. Biol Rev Camb Philos Soc 91: 235–254

Hare JA (2014) The future of fisheries oceanography lies in the pursuit of multiple hypotheses. ICES J Mar Sci 71: 2343–2356

Hersbach H, Bell B, Berrisford P, Biavati G and others (2023) ERA5 monthly averaged data on pressure levels from 1940 to present. Copernicus Climate Change Service (C3S) Climate Data Store (CDS). https://doi.org/10.24381/cds.6860a573 (accessed 5 October 2023)

Hickey BM (1979) The California Current System — hypotheses and facts. Prog Oceanogr 8:191–279

Hitchman SM, Reyns NB, Thompson AR (2012) Larvae define spawning habitat of bocaccio rockfish *Sebastes paucispinis* within and around a large southern California marine reserve. Mar Ecol Prog Ser 465:227–242

Hjort J (1914) Fluctuations in the great fisheries of northern Europe viewed in the light of biological research. Rapp P-V Cons Perm Int Explor Mer 20:1–228

Hjort J (1926) Fluctuations in the year classes of important food fishes. J Cons Int Explor Mer 1:5–38

Holder AM, Field JC (2019) An exploration of factors that relate to the occurrence of multiple brooding in rockfishes (*Sebastes* spp.). Fish Bull 117:56–64

Houde ED (1987) Fish early life dynamics recruitment variability. Am Fish Soc Symp 2:17–29

Houde ED (2008) Emerging from Hjort's shadow. J Northwest Atl Fish Sci 41:53–70

Johnson DW (2006) Predation, habitat complexity, and variation in density-dependent mortality of temperate reef fishes. Ecology 87:1179–1188

Kashef NS, Sogard SM, Fisher R, Largier JL (2014) Ontogeny of critical swimming speeds for larval and pelagic juvenile rockfishes (*Sebastes* spp., family Scorpaenidae). Mar Ecol Prog Ser 500:231–243

Kataoka T, Hinata H, Nihei Y (2013) Numerical estimation of inflow flux of floating natural macro-debris into Tokyo Bay. Estuar Coast Shelf Sci 134:69–79

Lefebvre LS, Beyer SG, Stafford DM, Kashef NS, Dick EJ, Sogard SM, Field JC (2018) Double or nothing: plasticity in reproductive output in the chilipepper rockfish (*Sebastes goodei*). Fish Res 204:258–268

Lenarz WH, Larson RJ, Ralston S (1991) Depth distributions of late larvae and pelagic juveniles of some fishes of the California Current. CCOFI Rep 32:41–46

Lett C, Roy C, Levasseur A, Van Der Lingen CD, Mullon C (2006) Simulation and quantification of enrichment and retention processes in the southern Benguela upwelling ecosystem. Fish Oceanogr 15:363–372

Love MS, Yoklavich MM, Thorsteinson L (2002) The rockfishes of the Northeast Pacific. University of California Press, Berkeley, CA

Lynn RJ, Simpson JJ (1987) The California Current System: the seasonal variability of its physical characteristics. J Geophys Res Oceans 92:12947–12966

Matsuzaki Y, Fujita I (2017) In situ estimates of horizontal turbulent diffusivity at the sea surface for oil transport simulation. Mar Pollut Bull 117:34–40

Miller RR, Field JC, Santora JA, Schroeder ID and others (2014) A spatially distinct history of the development of California groundfish fisheries. PLOS ONE 9:e99758

Mitarai S, Siegel DA, Watson JR, Dong C, McWilliams JC (2009) Quantifying connectivity in the coastal ocean with application to the Southern California Bight. J Geophys Res Oceans 114:1–21

Morales MM (2023) Physical–biological drivers of population replenishment for an ecologically important fish species of the California Current. PhD Dissertation, University of California, Santa Cruz, CA

Mori M, Mizobata K, Ichii T, Ziegler P, Okuda T (2022) Modeling the egg and larval transport pathways of the Antarctic toothfish (*Dissostichus mawsoni*) in the East Antarctic region: new insights into successful transport connections. Fish Oceanogr 31:19–39

Morrow R, Fu LL, Ardhuin F, Benkiran M and others (2019) Global observations of fine-scale ocean surface topography with the Surface Water and Ocean Topography (SWOT) Mission. Front Mar Sci 6:433647

Moser HG, Boehlert GW (1991) Ecology of pelagic larvae and juveniles of the genus *Sebastes.* Environ Biol Fishes 30:203–224

Nieto K, McClatchie S, Weber ED, Lennert-Cody CE (2014)

Effect of mesoscale eddies and streamers on sardine spawning habitat and recruitment success off southern and central California. J Geophys Res Oceans 119: 6330–6339

Nishimoto MM, Washburn L (2002) Patterns of coastal eddy circulation and abundance of pelagic juvenile fish in the Santa Barbara Channel, California, USA. Mar Ecol Prog Ser 241:183–199

Nishimoto MM, Simons RD, Love MS (2019) Offshore oil production platforms as potential sources of larvae to coastal shelf regions off southern California. Bull Mar Sci 95:535–558

NOAA National Centers for Environmental Information (2022) ETOPO 2022 30 arc-second global relief model. (accessed 7 August 2023)

Okubo A (1970) Horizontal dispersion of floatable particles in the vicinity of velocity singularities such as convergences. Deep-Sea Res Oceanogr Abstr 17:445–454

Owen R (1980) Eddies of the California Current System: physical and ecological characteristics. In: Power D (ed) The California islands: proceedings of a multidisciplinary symposium. Santa Barbara Museum of Natural History, Santa Barbara, CA, p 237–263

Pacific Fishery Management Council (2023) Pacific coast groundfish fisheries management plan for the California, Oregon and Washington groundfish fishery. Pacific Fishery Management Council. Portland, OR

Parrish RH, Nelson CS, Bakun A (1981) Transport mechanisms and reproductive success of fishes in the California Current. Biol Oceanogr 1:175–203

Pelc RA, Warner RR, Gaines SD, Paris CB (2010) Detecting larval export from marine reserves. Proc Natl Acad Sci USA 107:18266–18271

Petersen CH, Drake PT, Edwards CA, Ralston S (2010) A numerical study of inferred rockfish (*Sebastes* spp.) larval dispersal along the central California coast. Fish Oceanogr 19:21–41

Pineda J (1991) Predictable upwelling and the shoreward transport of planktonic larvae by internal tidal bores. Science 253:548–549

Pineda J, Hare JA, Sponaugle S (2007) Larval transport and dispersal in the coastal ocean and consequences for population connectivity. Oceanography (Wash DC) 20:22–39

Ralston S, Sakuma KM, Field JC (2013) Interannual variation in pelagic juvenile rockfish (*Sebastes* spp.) abundance—going with the flow. Fish Oceanogr 22:288–308

Rio MH, Mulet S, Picot N (2014) Beyond GOCE for the ocean circulation estimate: synergetic use of altimetry, gravimetry, and in situ data provides new insight into geostrophic and Ekman currents. Geophys Res Lett 41: 8918–8925

Sakuma KM, Ralston S, Roberts DA (1999) Diel vertical distribution of postflexion larval *Citharichthys* spp. and *Sebastes* spp. off central California. Fish Oceanogr 8: 68–76

Santora JA, Rogers TL, Cimino MA, Sakuma KM and others (2021) Diverse integrated ecosystem approach overcomes pandemic-related fisheries monitoring challenges. Nat Commun 12:6492

Schroeder ID, Santora JA, Bograd SJ, Hazen EL and others (2019) Source water variability as a driver of rockfish recruitment in the California Current Ecosystem: implications for climate change and fisheries management. Can J Fish Aquat Sci 76:950–960

Shen SG, Thompson AR, Correa J, Fietzek P, Ayón P, Checkley DM (2017) Spatial patterns of anchoveta (*Engraulis ringens*) eggs and larvae in relation to pCO_2 in the Peruvian upwelling system. Proc R Soc B 284:20170509

Sinha A, Balwada D, Tarshish N, Abernathey R (2019) Modulation of lateral transport by submesoscale flows and inertia-gravity waves. J Adv Model Earth Syst 11: 1039–1065

Stachura MM, Essington TE, Mantua NJ, Hollowed AB and others (2014) Linking Northeast Pacific recruitment synchrony to environmental variability. Fish Oceanogr 23: 389–408

Stockhausen WT, Hermann AJ (2007) Modeling larval dispersion of rockfish: a tool for marine reserve design? In: Heifetz J, DiCosimo J, Gharrett AJ, Love MS, O'Connell T, Stanley R (eds) Biology, assessment, and management of North Pacific rockfishes. Alaska Sea Grant College Program AK-SG-07-01. University of Alaska, Fairbanks, AK, p 251–273

Swalethorp R, Landry MR, Semmens BX, Ohman MD, Aluwihare L, Chargualaf D, Thompson AR (2023) Anchovy boom and bust linked to trophic shifts in larval diet. Nat Commun 14:7412

Taylor CA, Watson W, Chereskin T, Hyde J, Vetter R (2004) Retention of larval rockfishes, *Sebastes*, near natal habitat in the Southern California Bight, as indicated by molecular identification methods. CCOFI Rep 45:152–166

Thompson AR, Hyde JR, Watson W, Chen DC, Guo LW (2016) Rockfish assemblage structure and spawning locations in southern California identified through larval sampling. Mar Ecol Prog Ser 547:177–192

Thompson AR, Chen DC, Guo LW, Hyde JR, Watson W (2017) Larval abundances of rockfishes that were historically targeted by fishing increased over 16 years in association with a large marine protected area. R Soc Open Sci 4:170639

Wells BK, Schroeder ID, Bograd S, Hazen EL and others (2017) State of the California current 2016–2017: still anything but "normal" in the north. CCOFI Rep 58:1–55

White JW, Schroeger J, Drake PT, Edwards CA (2014) The value of larval connectivity information in the static optimization of marine reserve design. Conserv Lett 7: 533–544

Zaba KD, Franks PJS, Ohman MD (2021) The California undercurrent as a source of upwelled waters in a coastal filament. J Geophys Res Oceans 126:e2020JC016602

Editorial responsibility: Scott C. Burgess, Tallahassee, Florida, USA
Reviewed by: M. Clavel-Henry and 2 anonymous referees

Submitted: February 24, 2024
Accepted: September 18, 2024
Proofs received from author(s): November 14, 2024